

Plasma Polymerization of Organosiloxanes

SHIDE CAI, JIANGLIN FANG, and XUEHAI YU*

Centre of Materials Analysis, Department of Chemistry, Nanjing University,
Nanjing, 210008, People's Republic of China

SYNOPSIS

Plasma polymerization of disiloxanes containing various functional groups—hexamethyldisiloxane (HMDSO), tetramethyl-1,3-bis(chloromethyl)-disiloxane (CMDSO), tetramethyl-1,3-bis(hydroxylbutyl)-disiloxane (HBDSO), and tetramethyl-1,3-bis(amino propyl)-disiloxane (APDSO)—was carried out using an inductively coupled electrodeless glow discharge. The monomer polymerization kinetics and the distribution of chemical species deposited showed that monomer reactivity varied among the different siloxanes. Monomers of APDSO and CMDSO possessed higher rates of polymerization. Polymer IR spectra and ESCA analyses indicated that the chemical structures of plasma-polymerized products of HMDSO, HBDSO, and CMDSO resembled that of crosslinked polydimethylsiloxane. The polar hydroxyl and chlorine functionality in the HBDSO and CMDSO monomers was not present in the deposited films. In contrast, the polymerized product of APDSO retained amino functionality and also formed new Si-H bonds.

INTRODUCTION

Since Goodman¹ reported the glow discharge polymerization of styrene in the vapor phase plasma polymerization has been studied by many authors.²⁻⁵ The films produced by this technique are usually insoluble, pinhole free, and adhere well to substrates. Glow discharge polymerization is regarded as a unique polymer-forming technique. In plasma polymerization the free electrons gain energy from an imposed electrical field, and the transfer of energy to neutral gas molecules leads to the formation of many chemically reactive species, some of which result in plasma polymerization. Yasuda⁶ has proposed that plasma polymerization proceeds through a gradual propagation process. In plasma polymerization monomer molecules are split into various fragments. Since the radical concentration is very high, the combination of radical fragments predominates. However, this phenomenon does not stop polymer propagation reactions because the combined molecules can also be attacked. Through a continual cycle of initiation, combination, and reinitiation, macromolecules will finally form. Usually the reactiva-

tion of combined molecules occurs through the breaking of chemical bonds (such as C-H bonds) that are more sensitive to the plasma conditions. Therefore all the radical formation processes not accompanied by C-C bond breaking will accelerate the polymerization, and the monomer reactivity will be affected by its chemical structure.

In this work four organodisiloxanes with different functional groups—hexamethyldisiloxane (HMDSO), tetramethyl-1,3-bis(chloromethyl)-disiloxane (CMDSO), tetramethyl-1,3-bis(hydroxylbutyl)-disiloxane (HBDSO), and tetramethyl-1,3-bis(aminopropyl)-disiloxane (APDSO)—were polymerized by means of an inductively coupled electrodeless glow discharge. Through the determination of monomer polymerization kinetics, the effect of different chemical bonds in the monomer structures on monomer reactivity was investigated. The effects of the functional groups on the final structures of plasma polymerized films was examined using FT IR and ESCA techniques.

EXPERIMENTS

Materials

The monomers used for plasma polymerization included:

* To whom correspondence should be addressed.

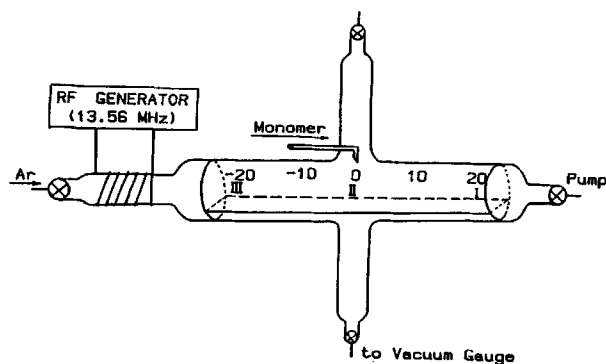


Figure 1 Plasma polymerization apparatus.

Hexamethyldisiloxane (HMDSO) purchased from Nanjing Paints Manufactory and used without further purification. Tetramethyl-1,3-bis(hydroxybutyl)-disiloxane (HBDSO) and tetramethyl-1,3-bis(aminopropyl)-disiloxane (APDSO) were purchased from Silar Laboratories Inc., and used without further purification. Tetramethyl-1,3-bis(chloromethyl)-disiloxane (CMDSO) was prepared by hydrolysis of dimethyl-chloromethyl-chlorosilane, which was made by chlorination of trimethylchlorosilane.⁶

Plasma System and Plasma Polymerization

Figure 1 shows the experimental apparatus that was equipped with a radio frequency (RF) (13.56 MHz) power generator, which can create an inductively coupling electrodeless glow discharge. A glass tubular reactor 9 cm in diameter and 40 cm in length was evacuated from the right side using a cold trap and rotary vacuum pump. The pressure in the system was monitored by a vacuum gauge during the plasma polymerization process. The coupling coil for glow discharge was placed at the left side of the reactor, and the monomer vapor was supplied to the center of reactor. A glass plate (length of 40 cm) within the reactor was overlaid with a number of microscope cover slides ($2.0 \times 2.0 \text{ cm}^2$) and placed at different positions from the extreme left (-20 cm) to right (+20 cm) in the reactor. The monomer vapor inlet position is defined as the zero position. The polymer deposition was measured gravimetrically. By the use of multiple glass slides the distribution of polymer deposition within the reactor could be calculated. The rate of monomer polymerization could be determined by the weight increment per unit time per unit area ($\text{mg}/\text{cm}^2 \text{ min}$).

The experimental procedures for plasma polymerization are similar to those reported elsewhere.⁷

The system was first evacuated by the rotary vacuum pump until a pressure of 0.02 mm Hg was achieved. Argon gas was then introduced into the reactor to displace the residual gases. Evacuation and argon introduction was repeated several times. The system was then again evacuated to 0.02 mm Hg, and monomer gas stored in a reservoir was bled into the reactor to replace the Ar. This process was also repeated several times. Finally, the pressure was controlled at 0.20 mm Hg by appropriate opening of the monomer inlet valve. Imposition of 30 W of RF power created the condition under which plasma polymerization was carried out.

IR (Infrared) Spectroscopy

Samples for infrared spectroscopy were scraped from slides using a knife, and were incorporated into KBr disks. Since the tubular reactor was comparatively long (40 cm length), the strength of glow discharge varied with position. It was noticed that the glow discharge was stronger near the tail of discharge coil (position I). IR spectra of samples deposited were determined from the material on slides at the right side of reactor (low-energy region), i.e., position I; the monomer vapor inlet area (middle-energy region), i.e., position II; and the tail area of coupling coil (high-energy region), i.e., position III.

The IR spectra were obtained on a Nicolet 170 SX FT-IR spectrometer.

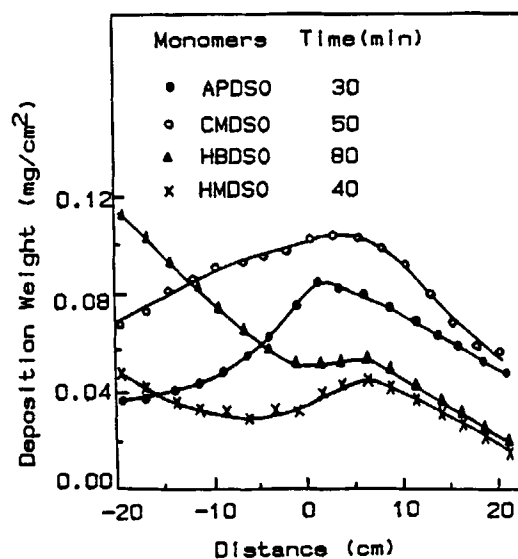


Figure 2 Distribution of polymer deposition with axial length in the reactor for the four organosiloxane monomers polymerized. Each reaction was carried out at a power of 30 W and a pressure of 0.20 mm Hg.

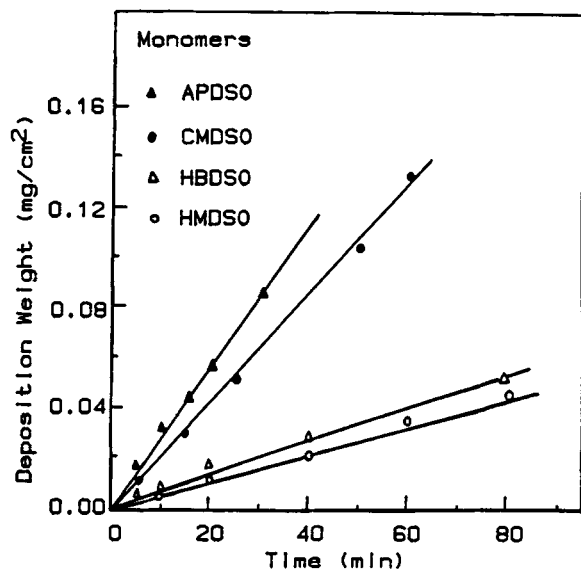


Figure 3 Plots of polymer deposition weight versus deposition time for the four organosiloxane monomers polymerized. The plasma reactor was maintained at a power of 30 W and a pressure of 0.20 mm Hg. The deposition rates were measured at position zero.

ESCA Spectra

Measurements of ESCA spectra were made on the polymers deposited on slides located at position II. The spectra were obtained using a VG ESCALAB MK-II electron spectrometer with X-ray gun operating at 15 kV and 10 mA. The data system of the meter was used to resolve the resulting complex spectra of the C_{1s} and Si_{2p} core levels.

RESULTS AND DISCUSSION

Distribution of Polymer Deposition and Polymerization Rates

Figure 2 shows the polymer deposition for the four monomers: APDSO, CMDSO, HBDSO, and HMDSO. As shown in the figure, the profile of polymer deposition varies with monomer type. The more reactive monomers yield a polymer deposition peak near the monomer inlet position. The distance between the deposition that occurs at the monomer inlet position (zero position) and the peak values

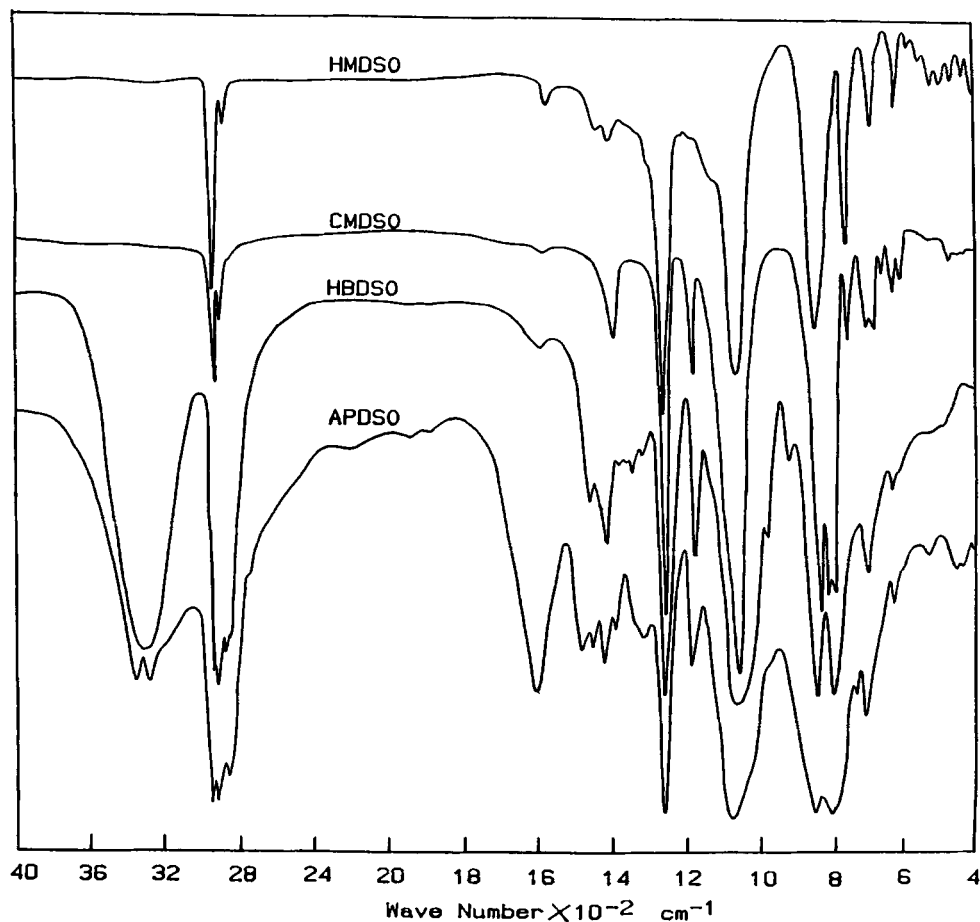


Figure 4 IR spectra of the four organosiloxane monomers.

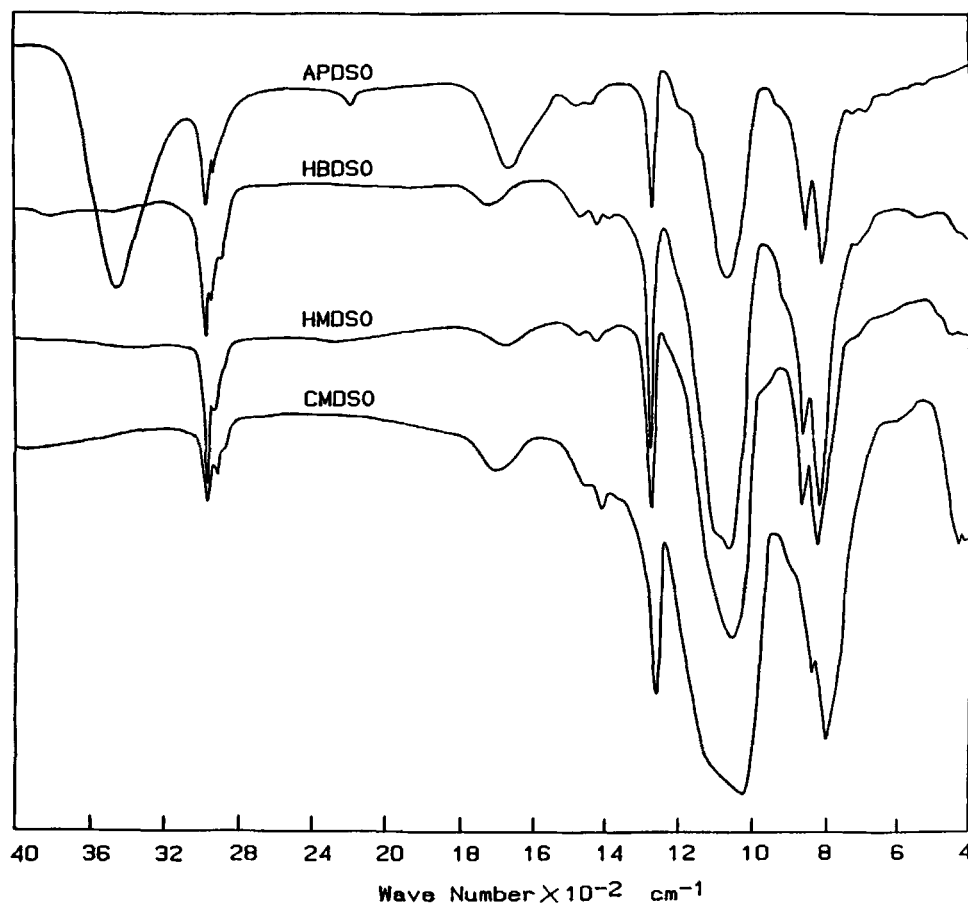


Figure 5 IR spectra of the plasma polymers derived from the four organosiloxane monomers.

that occur between 0 and 10 cm corresponds roughly to the monomer reactivity in the order from high to low: APDSO, CMDSO, HBDSO, HMDSO.

The polymerization rates could also be determined by measuring the weight of polymer deposited per unit area as a function of time, as shown in Figure 3. Here the deposition was measured at position 0. The weight of polymer deposited increased linearly with the reaction time. The slopes in Figure 3 represent the values of monomer polymerization rates. The slope is higher for monomers of APDSO and CMDSO than for HBDSO and HMDSO. This result is consistent with the inference of monomer reactivity from the deposition profile described earlier.

Figure 2 also shows that the higher reactivity monomers, APDSO and CMDSO, possessed a maximum in polymer deposition near the monomer inlet. This suggests that most of the monomer molecules polymerized just after they were injected into the reactor. However, monomers HBDSO and HMDSO showed a different deposition profile. For the less

reactive monomers the deposition increased near the tail of the RF coil. This suggests that some of the unpolymerized monomer molecules or oligomers are further polymerized in the high-energy region

Table I Infrared Frequencies and Band Assignments

Frequency (cm ⁻¹)	Band Assignments
3400–3200 ^a	N—H
3300 ^b	O—H
2950–2850	C—H
2150 ^a	Si—H
1700	C=O
1260	Si—CH ₃
1180 ^c	CH ₂ Cl
1150–1000	Si—O—Si, Si—O—C
840, 830	Si—C

^a Only found in monomer APDSO or its polymers.

^b Only found in monomer HBDSO.

^c Only found in monomer CMDSO.

through cracking reactions. The products of these reactions, which possess a higher crosslink density, were also confirmed by IR spectroscopy as described in the following section.

IR Spectra

Figure 4 shows IR spectra of the four monomers (HMDSO, CMDSO, HBDSO, and APDSO). Figure 5 shows the plasma deposition products of each monomer at position II. The positions of the major peaks in the spectra and their assignments to specific groups are shown in Table I.⁸ As shown in Figure 5 for the monomers of HMDSO, CMDSO, and HBDSO, the IR spectra of their products were very similar even though the monomer structures had distinct differences in their IR spectra. Here the $-\text{OH}$ group (3300 cm^{-1}) of HBDSO and $-\text{CH}_2\text{Cl}$ group (1180 cm^{-1}) of CMDSO disappeared from the plasma-polymerized polymer spectra.⁵ The 1700 cm^{-1} absorption in the product spectra is due to fur-

ther reactions of trapped radicals with oxygen and water after the films are exposed to air.⁵

In the plasma polymer of APDSO, there are not only the spectral features already mentioned but also ($3300\text{--}3400\text{ cm}^{-1}$) absorption characteristic of the amine groups of the monomer. There is also an absorption band at 2150 cm^{-1} , a characteristic peak of the Si-H group, which might be due to an increased fragmentation of the monomer due to the presence of the $-\text{NH}_2$ group.⁹ The $-\text{NH}_2$ group in APDSO can produce a large amount of atomic hydrogen, which promotes monomer fragmentation. The 2150 cm^{-1} absorption was greater for the product analyzed nearer to the tail of the glow discharge coil, which is consistent with a higher degree of fragmentation in this high-energy region.

Comparing the absorption widths of Si-O-Si and Si-O-C bonds in the $1150\text{--}1050\text{ cm}^{-1}$ region for the different monomers shows that width of the peaks decreased in the order CMDSO, HMDSO, HBDSO, and APDSO. This suggests that some crosslinking

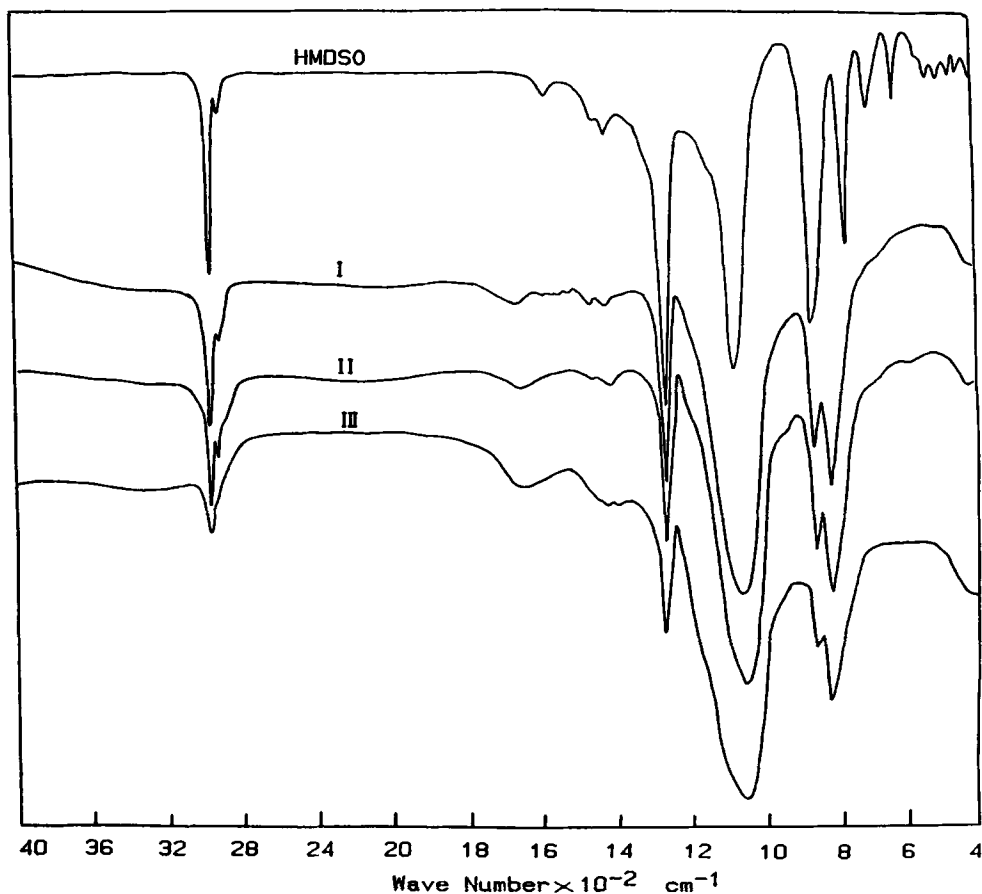


Figure 6 IR spectra of the monomer HMDSO and its plasma derived polymer at positions I, II, and III in the reactor (see Fig. 1).

reactions are occurring on the aliphatic chains of $-(\text{CH}_2)_4-$ and $-(\text{CH}_2)_3-$ units in the latter two monomers.

The IR spectra of plasma polymers deposited at positions I, II, and III are shown in Figure 6 for monomer HMDSO. Comparison of the spectra at position III with the spectra from positions I and II shows that the absorptions of C-H ($2950\text{--}2850\text{ cm}^{-1}$) and Si-CH₃ (1260 cm^{-1}) decreased, while the widths of Si-O-Si and Si-O-C absorptions ($1150\text{--}1050\text{ cm}^{-1}$) increased. This suggests that the degree of crosslinking increased in position III due to the higher degree of monomer fragmentation in this high-energy region.

ESCA Spectra

The ESCA analysis was carried out on plasma polymers deposited on slides located at position II. For the plasma polymers derived from HMDSO, HBDSO, and CMDSO, O_{1s}, C_{1s}, Si_{2s}, and Si_{2p} core levels were observed in the ESCA spectra. The plasma polymer obtained from the chlorine-containing monomer CMDSO exhibited no detectable chlorine in the ESCA spectra, which was consistent with the IR results. The plasma polymer of APSO had, in addition to the core level peaks mentioned, also the N_{1s} core level peak. This observation confirmed the presence of amino groups in the polymer product.

The C_{1s} and Si_{2p} peak regions in the spectra were resolved into two curves using a curve-fitting procedure,¹⁰ with the results listed in Table II. Each Si_{2p} core level peak was composed of two peaks consisting of Si-C (101.5 eV) and Si-O (102.5 eV). The C_{1s} was composed of two peaks consisting of aliphatic carbon, C-Si (284.5 eV) and C-O and/or C-N (285.9 eV).

Table II ESCA Spectra of Plasma Polymers for C_{1s}, Si_{2p}

Monomer	C _{1s}		Si _{2p}	
	C-C, C-Si (284.5 eV) (%)	C-O/C-N (285.9 eV) (%)	Si-C (101.5 eV) (%)	Si-O (102.5 eV) (%)
CMDSO	87	13	51	49
HMDSO	82	18	57	43
HBDSO	78	22	62	38
APDSO	85	15	82	18

The ratio of Si-C/Si-O is 3 : 1 in all four monomers. For the polymer produced from APDSO, the ratio of Si-C/Si-O is significantly increased, which suggests that the amino groups in the disiloxane facilitated the breaking of the Si-O bond rather than the Si-C bond during plasma fragmentation. On the other hand, for the polymers derived from CMDSO, HMDSO, and HBDSO, the ratios of Si-C/Si-O were decreased, suggesting that the breaking of the Si-C bond was predominant during polymerization. These results are consistent with the IR data, which showed that the polymers from CMDSO, HMDSO, and HBDSO possessed broader Si-O-Si and Si-O-C absorption bands.

CONCLUSIONS

1. Plasma polymerization kinetics of siloxane-containing monomers shows that monomers containing different functional groups possess different reactivities during plasma polymerization. In plasma polymerization, monomer molecules undergo partially selective chemical bond breaking and recombination processes to form macromolecules. The monomers of APDSO and CMDSO, which contain $-\text{NH}_2$ and $-\text{Cl}$ groups, respectively, exhibit high plasma polymerization rates compared to monomers HBDSO and HMDSO.

2. Monomers that possess different plasma reactivity yield different polymer deposition profiles. The more active APDSO and CMDSO monomers produce polymers that deposit mainly near the monomer inlet. This gives rise to a deposition peak in region II. The less active HBDSO and HMDSO monomers allow reactive oligomers to escape the monomer inlet area and further polymerize in the higher energy region III.

3. IR and ESCA spectra analyses show that monomers of HMDSO, CMDSO, and HBDSO give similar products that resemble the chemical structure of crosslinked polydimethylsiloxane. The $-\text{OH}$ and $-\text{Cl}$ groups in monomers disappear from the polymerized products. In contrast for the monomer APDSO amine groups appear in the product as well as new Si-H bonds. A high degree of APDSO monomer fragmentation is suggested to occur under the plasma reaction conditions.

Support for this work was provided by National Science Foundation of the People's Republic of China. We also express our appreciation to Dr. S. L. Cooper of UW Madison for his review of this manuscript.

REFERENCES

1. J. Goodman, *J. Polym. Sci.*, **1**, 551-552 (1960).
2. J. R. Hollahan and A. T. Bell, *The Techniques and Applications of Plasma Chemistry*, Wiley-Interscience, New York, 1974.
3. M. Shen and A. T. Bell, *Plasma Polymerization*, ACS Symp. Ser., **108**, 1-33 (1978).
4. H. Yasuda, *J. Appl. Polym. Sci.: Appl. Polym. Symp.*, *Plasma Polymerization and Plasma Treatment*, Vol. 38, Wiley, New York, 1984.
5. H. Yasuda, *J. Polym. Sci.-Macromol. Rev.*, **16**, 199-293 (1981).
6. John L. Speier, *J. Am. Chem. Soc.*, **73**(1), 824 (1951).
7. Shide Cai, Xuehai Yu, and Jianglin Fang, *Chinese J. Appl. Chem.*, **4**(6), 76-78 (1987).
8. Jiro Sakata, Minoru Yamamoto, and Masana Hirai, *J. Appl. Polym. Sci.*, **31**, 1999 (1986).
9. A. M. Wrobel and M. Kryzanski, *J. Macromol. Sci.-Chem.*, **A12**(7), 1041 (1978).
10. N. Inagaki and A. Kishi, *J. Polym. Sci.-Polym. Chem. Ed.*, **21**, 1335 (1983).

Received January 28, 1991

Accepted February 21, 1991